Detection of Mercury(II) by Quantum Dot/DNA/Gold Nanoparticle Ensemble Based Nanosensor Via Nanometal Surface Energy Transfer

ARTICLE *in* ANALYTICAL CHEMISTRY · AUGUST 2011

Impact Factor: 5.64 · DOI: 10.1021/ac2019014 · Source: PubMed

5 AUTHORS, INCLUDING:

Xiaodong Shi
University of South Florida
107 PUBLICATIONS **2,817** CITATIONS
SEE PROFILE

Lawrence A. Hornak
West Virginia University
135 PUBLICATIONS **1,288** CITATIONS
SEE PROFILE

analytical chemistry

ARTICLE

pubs.acs.org/ac

Detection of Mercury(II) by Quantum Dot/DNA/Gold Nanoparticle Ensemble Based Nanosensor Via Nanometal Surface Energy Transfer

Ming Li,[†] Qiaoyi Wang,[‡] Xiaodong Shi,[‡] Lawrence A. Hornak,[§] and Nianqiang Wu*[,†]

[†]Department of Mechanical and Aerospace Engineering, WVNano Initiative, [‡]Eugene Bennett Department of Chemistry, and [§]Lane Department of Computer Science and Electrical Engineering, West Virginia University, Morgantown, West Virginia 26506, United States

Supporting Information

ABSTRACT:

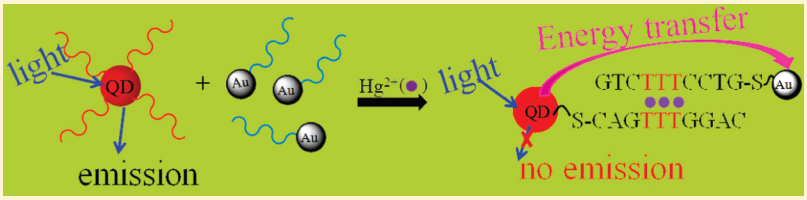

An ultrasensitive fluorescent sensor based on the quantum dot/DNA/gold nanoparticle ensemble has been developed for detection of mercury(II). DNA hybridization occurs when Hg(II) ions are present in the aqueous solution containing the DNA-conjugated quantum dots (QDs) and Au nanoparticles. As a result, the QDs and the Au nanoparticles are brought into the close proximity, which enables the nanometal surface energy transfer (NSET) from the QDs to the Au nanoparticles, quenching the fluorescence emission of the QDs. This nanosensor exhibits a limit of detection of 0.4 and 1.2 ppb toward Hg(II) in the buffer solution and in the river water, respectively. The sensor also shows high selectivity toward the Hg(II) ions.

Mercuric ion (Hg^{2+}) is one of the most toxic heavy metals and a kind of persistent contaminant that is not biodegradable and thus is retained in the ecosystem.[1−3] Moreover, Hg^{2+} can accumulate in vital organs through the food chain and cause human illness and dysfunction, posing a threat to human health, animals, plants, and the planet itself. Conventional analytical techniques including cold-vapor atomic fluorescence spectrometry (CV-AFS),[4] cold-vapor atomic absorption spectrometry (CV-AAS),[5] inductively coupled plasma-mass (ICPMS),[6] ultraviolet−visible spectrometry, and X-ray absorption spectroscopy[7] have been extensively used for measurement of Hg^{2+} in water samples. However, these methods are labor-intensive, time-consuming, and laboratory-based and require large sample volume. Furthermore, they cannot be used for on-site detection of Hg^{2+} in the environment. Therefore, there is a strong incentive to develop a sensitive, reliable, and convenient approach for monitoring Hg^{2+} in the environment.[1] Much effort has been made to develop portable sensors, including fluorescent sensors based on organic fluorophores and conjugated polymers, scanometric sensors, and colorimetric sensors.[8−11] Special attention has been paid to the sensors based on Förster resonance energy transfer (FRET) between a fluorescent donor and an acceptor.[12−16] Generally, organic dyes are used as the energy donor and the energy acceptor in FRET sensors.

Recently, the organic energy acceptor was replaced with a gold nanoparticle (Au NP) although the energy donor still was the organic dye, which rendered the nanometal surface energy transfer (NSET) mechanism, leading to a high energy transfer rate from the organic donor to the Au NP acceptor and a long quenching distance.[17−23] It would be of significance to eliminate the organic dyes that are present in the above-mentioned FRET and NSET sensors, because the use of organic dyes results in photobleaching, low sensitivity, and poor reproducibility.

It is well-known that semiconductor quantum dots (QDs) are attractive fluorescent labels due to their high quantum efficiency, photostability, and size-tunable optical properties as compared to conventional organic dyes.[24−29] In the present work, QDs and Au NPs are used to create a NSET sensor for Hg^{2+} detection in water. It is found that this kind of sensor provides high sensitivity and selectivity for Hg^{2+} detection.

EXPERIMENTAL SECTION

Materials. Cadmium oxide (CdO, 99.99+%), zinic oxide (ZnO, 99.99%), sulfur (powder, 99.98%), trioctylphosphine oxide (TOPO, tech. 90%), 1-octadecene (ODE, tech. 90%), oleic acid (tech. 90%), octyldecylamine (ODA, tech. 90%), trioctylphosphine (TOP, tech. 90%), selenium (powder, 99+%), *p*-mercaptobenzoic acid (MBA, tech. 90%), 3-mercaptopropionic acid (MPA, 99+%), $Cu(NO_3)_2$, $Hg(NO_3)_2$, $(HgNO_3)_2 \cdot 2H_2O$, $Pb(NO_3)_2$ (99.995%), $Cd(NO_3)_2 \cdot 4H_2O$, and 5 M NaCl stock solution were purchased from Sigma-Aldrich. *n*-Tetradecylphosphonic acid (TDPA) was purchased from PCI Synthesis. Methylene dichloride (CH_2Cl_2, HPLC grade), methanol (ACS grade), and

Received: May 16, 2011
Accepted: August 15, 2011
Published: August 15, 2011

acetone (ACS grade) were purchased from Fisher Scientific. Chloroauric acid trihydrate ($HAuCl_4 \cdot 3H_2O$), $NaBH_4$ (98%), KI (99.9%), $AgNO_3$ (Premion, 99.995%), and ethylenediamine (99%) were obtained from Alfa-Aesar. All chemicals and solvents were obtained from the commercial sources and used directly without further purification, and all glassware was cleaned successively with aqua regia and D.I. water and then dried before use.

Preparation of DNA-Functionalized CdSe/ZnS QDs and Au NPs. TOPO-QDs were synthesized by the well-established method with a slight modification.[30,31] Briefly, a mixture of 0.0514 g of CdO, 0.2232 g of TDPA, 1.0 g of ODA, and 2.5 g of TOPO was heated to 300 °C under a Ar flow to obtain a colorless clear solution and then lowered to 260 °C for the injection of the TOPSe solution (0.0665 g of Se in 2.4 mL of TOP). The temperature was kept at 240 °C for the growth of the desired CdSe nanocrystals. The 0.1 M Zn-containing stock solution was made by 0.407 g of ZnO in 20 mL of oleic acid and 30 mL of ODE. The 0.1 M S-containing stock solution was made by 0.16 g of S in 50 mL of ODE. Once the CdSe nanocrystals with the desired fluorescence emission was observed, the temperature was lowered to about 220 °C, and the calculated amount of the Zn- or S-stock solutions for each ZnS monolayer were alternately injected. After that, the resulting CdSe/ZnS nanocrystals were purified by methanol and acetone, followed by the ligand exchange with MPA to prepare the water-soluble QDs. Capping of the QDs with MPA made the QDs water-soluble and dispersed in the aqueous solution up to one month.

The 3 nm sized Au NPs were prepared through the reduction of $HAuCl_4 \cdot 3H_2O$ by $NaBH_4$.[32] The water-soluble QDs and Au NPs were functionalized by two complementary ssDNA except for three deliberately designed T−T mismatches (5′-HS-CAGTTTGGAC-3′ and 5′-HS-GTCCTTTCTG-3′), respectively.[33,34] The average DNA loadings of the resulting DNA-functionalized QDs and Au NPs (Probe A: QD-S-CAGTTTGGAC-3′ and Probe B: Au-S-GTCCTTTCTG-3′) were four DNAs per QD and one DNA per Au NP based on the optical absorption spectra.

Hg^{2+} Detection. The DNA/QD stock solution was diluted to 30 mL using the PBS buffer. Afterward, 8 mL of diluted DNA/QD solution, 4 mL of 0.3 M PBS solution (10 mM NaH_2PO_4/Na_2HPO_4 and 0.3 M NaCl), and 0.5 mL of DNA/Au NPs were mixed, followed by addition of 10 mM ethylenediamine PBS stock solution and 5 M NaCl. This resulted in the test solution.

The test was conducted in a PBS solution that contained 96 nM DNA/QDs, 104 nM DNA/Au NPs, 0.1 mM ethylenediamine, 10 mM NaH_2PO_4/Na_2HPO_4, and 0.3 M NaCl. After Hg^{2+} ions were added into the test solution (1 μM Hg^{2+}), the time-dependent fluorescence emission intensity at 572 nm was monitored to determine the hybridization kinetics.

For the sensitivity measurement, different concentrations of Hg^{2+} (0, 1, 2, 3, 4, 5, 6, 8 10, 15, 20, 30, 40, 60, 80, 100, 200, 500, and 1000 nM) were added. The fluorescence emission spectra were then monitored.

For the selectivity measurement, various metal ions of 100 nM were supplied with their salts (KI, $AgNO_3$, $(HgNO_3)_2 \cdot 2H_2O$, $CaCl_2$, $Cd(NO_3)_2 \cdot 4H_2O$, $Cu(NO_3)_2$, $Hg(NO_3)_2$, and $Pb(NO_3)_2$). The fluorescence emission spectra were monitored after the introduction of metal ions into the test assay.

The river water sample was taken from the Monongahela River and then filtered with the filter paper (Millipore, Isopore membrane), and then, 8 mL of DNA/QD solution, 4 mL of filtered river water, and 0.5 mL of DNA/Au NP solution were mixed, followed by the measurement of various concentrations of Hg^{2+} according to the same procedure as shown above.

Characterization. The size of QDs and Au nanoparticles was observed under a transmission electron microscope (TEM) with a JEM 2100F operated at 200 kV. The TEM specimens were prepared by dropping the Au NP solution onto a carbon-coated copper grid and then dried in air. UV−visible absorption spectra were recorded in the range of 200−800 nm with the Shimadzu UV-2550 spectrometer (Japan). The fluorescence (FL) emission spectra were measured using a HITACHI F-7000 fluorescence spectrophotometer with the excitation of 400 nm. X-ray photoelectron spectra (XPS) were measured with PHI 5000 Versa Probe system (Physical Electronics, MN). The obtained spectra were calibrated with the reference to the C 1s peak of aliphatic carbon at 284.8 eV.

RESULTS AND DISCUSSION

Figure 1a schematically shows the design of the NSET sensor. First, two probes (Probe A: QD-S-CAGTTTGGAC-3′ and Probe B: Au-S-GTCCTTTCTG-3′) were prepared by functionalization of the 3.8 nm sized water-soluble CdSe/ZnS core−shell QDs and the 3 nm sized Au NPs with single-stranded DNA (ssDNA) sequences of 5′-HS-CAGTTTGGAC-3′ and 5′-HS-GTCCTTTCTG-3′, respectively. These two ssDNA strands are complementary except for three deliberately designed T−T mismatches. In the absence of Hg^{2+}, Probe A and Probe B are not capable of hybridization and dispersed in the aqueous solution due to the electrostatic repulsion from the negatively charged ssDNA attached on the nanoparticle surfaces. In this case, Probe A will fluoresce at 572 nm under an excitation laser. When Hg^{2+} ions are present, DNA hybridization will occur due to the formation of thymine−Hg^{2+}−thymine (T−Hg^{2+}−T) complexes.[35] As a result, QDs and Au NPs will be brought into close proximity, which enables quenching of the fluorescence emission of the QDs (Figure 1a,b). Visual examination showed that the brightness of the QD/DNA/Au NP solution diminished remarkably after addition of 1 μM Hg^{2+} ions (Figure 1c). The further experiment indicated that there was no observable change in the fluorescence emission intensity when Hg^{2+} was added to the solution containing only QDs in the absence of the Au NPs (Figure S8 in Supporting Information). Therefore, quenching of the fluorescence emission of QDs was due to the presence of the Au NPs rather than the addition of the Hg^{2+} ions.

Generally, the fluorescence emission of the quantum dots could be quenched by the proximal gold nanoparticle via two possible mechanisms, that is, charge transfer (such as Dexter[36,37]) and energy transfer (such as FRET[12−16] and NSET[17−22]). In the Dexter mechanism, charge carriers are exchanged between the donor and the acceptor, which requires the overlap of the wave functions between the donor and the acceptor. The rate of charge transfer decreases exponentially as the distance, following the relation of $\exp[-(2r/L)]$, where r is the edge-to-edge distance between the donor and the acceptor and L is the sum of the van-der Waals radii of the donor and the acceptor. Therefore, the rate of charge transfer drops to negligibly small values as the edge-to-edge distance increases more than one or two molecular diameters (0.5−1 nm). FRET originates from the dipole−dipole interaction, which requires the overlap of the emission band of the donor with the absorption band of the acceptor. The rate of energy transfer depends on the $1/d^6$ separation distance. The fluorescence emission of the donor could be quenched in the

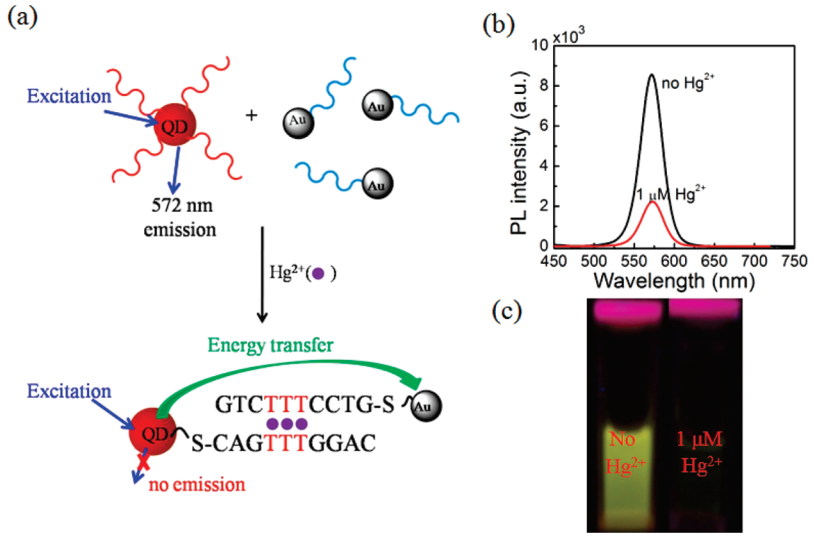

Figure 1. (a) Schematic illustration of the operating principle of the QD/DNA/Au NP ensemble sensor for Hg^{2+} detection. (b) Fluorescence emission spectra and (c) photograph under 365 nm laser excitation of the QD/DNA/Au NP solution (96 nM QDs, 104 nM Au NPs, and 0.1 mM ethylenediamine in 0.3 M PBS) before and after addition of 1 μM Hg^{2+}.

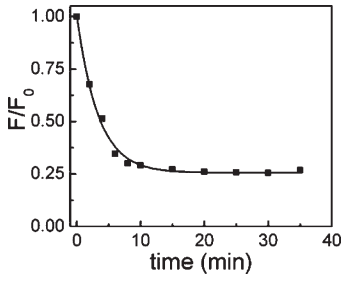

Figure 2. Time-dependent fluorescence emission intensity (572 nm) of the QD/DNA/Au NP system at 1 μM Hg^{2+} concentration (96 nM CdSe/ZnS QDs, 104 nM Au NPs, and 0.1 mM ethylenediamine in 0.3 M PBS).

separation distance up to 10 nm. NSET does not require a resonant interaction between the electrons but rather an interband electronic transition, which is described by the theory of Perrson.[38] The rate of energy transfer decreases with a $1/d^4$ distance dependence. NSET typically shows longer energy transfer distance than FRET. Willner et al. claimed that the quenching of quantum dots (QDs) was ascribed to the electron transfer from the QD to metallic ions.[39] In the present work, it is believed that the fluorescence emission of the quantum dots was quenched by the gold nanoparticle via the NSET mechanism. The details of results have been published somewhere else.[40] Our results show that the efficiency of quenching followed a $1/d^4$ distance dependence instead of the exponential relation. The fluorescence emission of the quantum dots was quenched by the gold nanoparticle at the separation distance up to ~6.2 nm, which was much longer than the typical quenching distance in the Dexter mechanism.

The hybridization kinetics of Probe A and Probe B was monitored in the phosphate buffered saline (0.3 M PBS) solution (pH = 7.0) containing 10 mM NaH_2PO_4/Na_2HPO_4 and 0.3 M NaCl in the presence of 1 μM Hg^{2+} at room temperature (Figure 2). It was found that it took about 10 min to accomplish DNA hybridization through the coordinating interaction between Hg^{2+} and the thymine base. The assay time was shorter than the results reported previously.[34]

To evaluate the sensitivity of the NSET sensor, the fluorescence emission intensity of the assay was measured after addition of various concentrations of Hg^{2+} ions (0, 1, 2, 3, 4, 5, 6, 8, 10, 15, 20, 30, 40, 60, 80, 100, 200, 500, and 1000 nM) (Figure 3). As shown in Figure 3a,b, the intensity of fluorescence emission was very sensitive to the change in the Hg^{2+} concentration and decreased as an increase in the Hg^{2+} concentration. The fluorescence quenching efficiency was quantified by the equation ($I = (F_o - F)/F_o$), where F_o and F were the fluorescence intensity at 572 nm before and after Hg^{2+} addition, respectively. A linear correlation of the fluorescence quenching efficiency with the Hg^{2+} concentration was observed in the Hg^{2+} concentration range from 2 nM to 60 nM (Figure 3c). The international World Health Organization (WHO) and the U.S. Environmental Protection Agency (EPA) regulate the maximum allowable levels of Hg^{2+} in drinking water to be 6 and 2 ppb, respectively. The present method enabled the efficient detection of Hg^{2+} in water with an ultralow limit of detection (LOD) of 2 nM (0.4 ppb), which was lower than both the WHO and EPA standards. The high sensitivity could be attributed to the efficient fluorescence quenching by coupling of several Au NPs to one QD. The LOD of the present NSET mercury sensor was improved in comparison with those of the previously reported colorimetric sensor (LOD = 3 μM)[11] and the FRET sensor (LOD = 40 nM)[35] although all these three types of sensors had the similar molecular recognition probe, i.e., the DNA containing the $T-Hg^{2+}-T$ coordination.

The selectivity of the NSET sensor was investigated by testing the fluorescence quenching efficiency in the presence of other environmental metal ions, including K^+, Ag^+, Hg^+, Ca^{2+}, Cd^{2+}, Cu^{2+}, and Pb^{2+}. At first, the fluorescence quenching efficiency was measured upon addition of a single type of 100 nM metal ions into the 0.3 M PBS solution (Figure 4). The result showed excellent selectivity toward Hg^{2+} over other metal ions including Hg^+. The excellent selectivity for Hg^{2+} was attributed to its specific chelating ability with DNA through the formation of $T-Hg^{2+}-T$ complexes.[35,41] Furthermore, to test the anti-interference capability, the fluorescence quenching efficiency of the assay was measured in the PBS solution in which Hg^{2+} coexisted with the mixture of K^+, Ag^+, Hg^+, Ca^{2+}, Cd^{2+}, Cu^{2+}, and Pb^{2+}

dx.doi.org/10.1021/ac2019014 |Anal. Chem. 2011, 83, 7061–7065

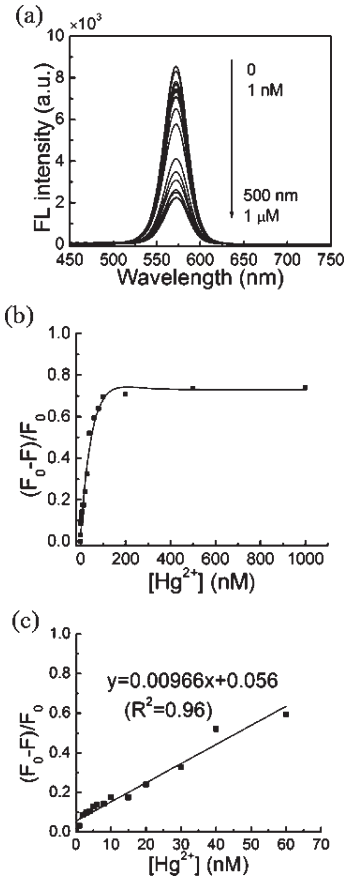

Figure 3. (a) Fluorescence emission spectra of the QD/DNA/Au NP system in 0.3 M PBS solution after addition of various concentrations of Hg^{2+} (0, 1, 2, 3, 4, 5, 6, 8, 10, 15, 20, 30, 40, 60, 80, 100, 200, 500, and 1000 nM) into the 0.3 M PBS solution (96 nM QDs, 104 nM Au NPs, and 0.1 mM ethylenediamine). (b) Plot of fluorescence quenching efficiency as a function of the Hg^{2+} concentration. (c) Linear region of (b).

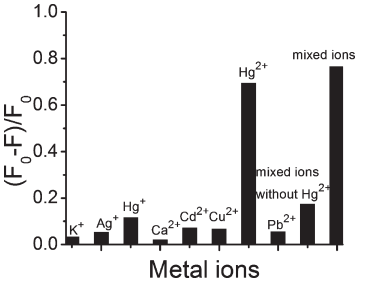

Figure 4. Fluorescence quenching efficiency in the presence of various metal ions. The concentration of each metal ion is 100 nM (96 nM QDs, 104 nM Au NPs, and 0.1 mM ethylenediamine in 0.3 M PBS).

ions (the concentration of each metal ion in the mixture was 100 nM) (Figure 4). Although the addition of the mixed metal ions without Hg^{2+} resulted in little higher fluorescence quenching than that of the individual metal ion, the fluorescence quenching efficiency was obviously far higher in the presence of Hg^{2+}. This indicated that the present nanosensor had strong anti-interference capability and excellent selectivity.

In order to test whether the NSET sensor is able to be used in the real-world water, the interference of unknown substances in

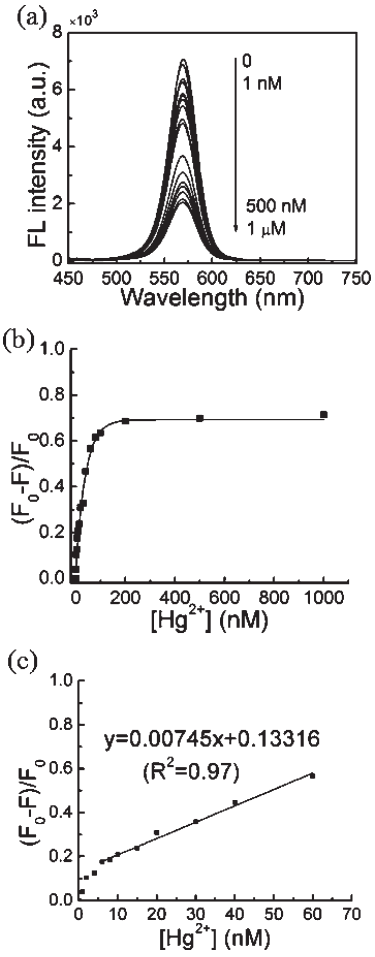

Figure 5. (a) Fluorescence emission spectra of the QD/DNA/Au NP system in river water containing various concentrations of Hg^{2+} (0, 1, 2, 4, 6, 8, 10, 15, 20, 30, 40, 60, 80, 100, 200, 500, and 1000 nM) (96 nM QDs, 104 nM Au NPs, 0.1 mM ethylenediamine, and 0.3 M NaCl in the mixture of the PBS with the river water). (b) Plot of the fluorescence quenching efficiency as a function of the Hg^{2+} concentration in river water. (c) Linear region of (b).

the river water on the fluorescence emission of nanosensor was evaluated with the water sample from the Monongahela River near our campus. Prior to testing, the river water was filtered by the filter paper (Millipore, Isopore membrane). The total mercury content in the filtered river water was measured to be <0.1 ppb by Agilent 7500ce inductively coupled plasma mass spectrometry (ICPMS). The filtered water was then mixed with the stock DNA/QD buffer solution in the ratio of 1:2 (v/v) to obtain the DNA/QD test solution. The sensitivity of the QD/DNA/Au/river water system was checked after addition of various concentrations of Hg^{2+} ions (0, 1, 2, 4, 6, 8, 10, 15, 20, 30, 40, 60, 80, 100, 200, 500, and 1000 nM). The initial fluorescence intensity in the DNA/QD solution containing the river water was lower than that in the pure buffer solution (Figure 5a), which was believed to be ascribed to the fluorescence quenching of the QDs by the various environmental substances in the river water. The fluorescence intensity of the assay decreased with an increase in the concentration of the added Hg^{2+} ions (Figure 5b). The sensitivity (the slope of the linear region) was a little lower, and the limit of detection increased to 6 nM (1.2 ppb) as compared to that (0.4 ppb) of the pure PBS assay (Figure 5c).

CONCLUSIONS

An ultrasensitive and highly selective nanosensor, which was based on the NSET in the QD/DNA/Au NP ensemble, has been successfully developed for Hg^{2+} detection in water. This sensor showed a limit of detection of 0.4 ppb in the buffer solution. The excellent selectivity toward Hg^{2+} was demonstrated in an aqueous solution in the presence of the other environmental metal ions. The developed nanosensor is expected to be used for on-site detection of mercury in a real aquatic environment due to a number of distinct advantages. First, the QD/Au optical assay eliminates the photobleaching problem that is usually associated with organic dyes. Second, individual QDs are bright fluorophores due to their high quantum yield, which enables the QD/Au assay to offer high sensitivity. Third, the QD/DNA/Au ensemble enables the NSET sensing mechanism. It has been reported that NSET has higher energy transfer efficiency and wider energy transfer distance than the conventional FRET.[17,42,43] Fourth, DNA as a molecular recognition probe is more stable in a nonphysiological solution than enzymes, proteins, and live microbes that are typically used as molecular recognition probes in biosensors. Finally, the design of our nanosensor system provides a potential capability of simultaneous and discriminative detection of several metal ions in a multianalyte sample through tuning the optical emission of quantum dots at various wavelengths. The fluorescence emissions of the multicolor QDs can be excited with a single laser at a wavelength far from the emission wavelengths of all the QDs. This is a significant advantage over the multiple light sources required to excite a series of organic dyes.

ASSOCIATED CONTENT

Supporting Information. TEM and XPS characterization of CdSe/ZnS quantum dots and Au nanoparticles; Figures S1−S9. This material is available free of charge via the Internet at http://pubs.acs.org.

AUTHOR INFORMATION

Corresponding Author

*Fax: (304)-293-6689. E-mail: nick.wu@mail.wvu.edu.

ACKNOWLEDGMENT

This work was financially supported by a NSF grant (CBET-0754405). The resource and facilities used were partially supported by NSF (EPS 1003907) and a Research Challenge Grant from the State of West Virginia (EPS08-01), the West Virginia University Research Corporation, and the West Virginia EPSCoR Office. We acknowledge use of the WVU Shared Research Facilities.

REFERENCES

(1) Nolan, E. M.; Lippard, S. J. *Chem. Rev.* **2008**, *108*, 3443–3480.
(2) Balaji, T.; El-Safty, S. A.; Matsunaga, H.; Hanaoka, T.; Mizukami, F. *Angew. Chem., Int. Ed.* **2006**, *45*, 7202–7208.
(3) Yilmaz, F.; Özdemir, N.; Demirak, A.; Tuna, A. L. *Food Chem.* **2007**, *100*, 830–835.
(4) Lorber, K. E. *Waste Manage. Res.* **1986**, *4*, 3–13.
(5) Kunkel, R.; Manahan, S. E. *Anal. Chem.* **1973**, *45*, 1465–1468.
(6) Bings, N. H.; Bogaerts, A.; Broekaert, J. A. C. *Anal. Chem.* **2006**, *78*, 3917–3946.
(7) Bernaus, A.; Gaona, X.; Esbrí, J. M.; Higueras, P.; Falkenberg, G.; Valiente, M. *Environ. Sci. Technol.* **2006**, *40*, 4090–4095.
(8) Lee, J.; Jun, H.; Kim, J. *Adv. Mater.* **2009**, *21*, 1–4.
(9) Lee, J.; Mirkin, C. A. *Anal. Chem.* **2008**, *80*, 6805–6808.
(10) Lee, J.; Han, M. S.; Mirkin, C. A. *Angew. Chem., Int. Ed.* **2007**, *46*, 4093–4096.
(11) Xue, X.; Wang, F.; Liu, X. *J. Am. Chem. Soc.* **2008**, *130*, 3244–3245.
(12) Roy, R.; Hohng, S.; Ha, T. *Nat. Methods* **2008**, *5*, 507–516.
(13) Goldman, E. R.; Medintz, I. L.; Whitley, J. L.; Hayhurst, A.; Clapp, A. R.; Uyeda, H. T.; Deschamps, J. R.; Lassman, M. E.; Mattoussi, H. *J. Am. Chem. Soc.* **2005**, *127*, 6744–6751.
(14) Zhang, X.; Xiao, Y.; Qian, X. *Angew. Chem., Int. Ed.* **2008**, *47*, 8025–8029.
(15) Davis, J. J.; Burgess, H.; Zauner, G.; Kuznetsova, S.; Salverda, J.; Aartsma, T.; Canters, G. W. *J. Phys. Chem. B* **2006**, *110*, 20649–20654.
(16) Ray, P. C.; Fortner, A.; Darbha, G. K. *J. Phys. Chem. B* **2006**, *110*, 20745–20748.
(17) Yun, C.; Javier, S. A.; Jennings, T.; Fisher, M.; Hira, S.; Peterson, S.; Hopkins, B.; Reich, N. O.; Strouse, G. F. *J. Am. Chem. Soc.* **2005**, *127*, 3115–3119.
(18) Kondon, M.; Kim, J.; Udawatte, N.; Lee, D. *J. Phys. Chem. C* **2008**, *112*, 6695–6699.
(19) Gill, R.; Willner, I.; Shweky, I.; Banin, U. *J. Phys. Chem. B* **2005**, *109*, 23715–23719.
(20) Dyadyusha, L.; Yin, H.; Jaiswal, S.; Brown, T.; Baumberg, J. J.; Booy, F. P.; Melvin, T. *Chem. Commun.* **2005**, 3201–3203.
(21) Darbha, G. K.; Ray, A.; Ray, P. C. *ACS Nano* **2007**, *1*, 208–214.
(22) Ye, B.; Yin, B. *Angew. Chem., Int. Ed.* **2008**, *47*, 8386–8389.
(23) Li, M.; Li, R.; Li, C. M.; Wu, N. Q. *Front. Biosci.* **2011**, *S3*, 1308–1331.
(24) Talapin, D. V.; Rogach, A. L.; Kornowski, A.; Haase, M.; Weller, H. *Nano Lett.* **2001**, *1*, 207–211.
(25) Peng, X.; Schlamp, M. C.; Kadavanich, A. V.; Alivisatos, A. P. *J. Am. Chem. Soc.* **1997**, *119*, 7019–7029.
(26) Kairdolf, B. A.; Smith, A. M.; Nie, S. *J. Am. Chem. Soc.* **2008**, *130*, 12866–12867.
(27) Zhao, H.; Chaker, M.; Wu, N. Q.; Ma, D. *J. Mater. Chem.* **2011**, *21*, 8898–8904.
(28) Wang, D.; Zhao, H.; Wu, N. Q.; El Khakani, A.; Ma, D. *J. Phys. Chem. Lett.* **2010**, *1*, 1030–1035.
(29) Tan, G. L.; Hommerich, U.; Temple, D.; Wu, N. Q.; Zheng, J. G.; Loutts, G. *Scr. Mater.* **2003**, *48*, 1469–1474.
(30) Xie, R.; Kolb, U.; Li, J.; Basché, T.; Mews, A. *J. Am. Chem. Soc.* **2005**, *127*, 7480–7488.
(31) Li, J. J.; Wang, Y. A.; Guo, W.; Keay, J. C.; Mishima, T. D.; Johnson, M. B.; Peng, X. *J. Am. Chem. Soc.* **2003**, *125*, 12567–12575.
(32) Chen, S.; Kimura, K. *Langmuir* **1999**, *15*, 1075–1082.
(33) Mitchell, G. P.; Mirkin, C. A.; Letsinger, R. L. *J. Am. Chem. Soc.* **1999**, *121*, 8122–8123.
(34) Maxwell, D. J.; Taylor, J. R.; Nie, S. *J. Am. Chem. Soc.* **2002**, *124*, 9606–9612.
(35) Ono, A.; Togashi, H. *Angew. Chem., Int. Ed.* **2004**, *43*, 4300–4302.
(36) Dexter, D. L. *J. Chem. Phys.* **1953**, *21*, 836–850.
(37) Inokuti, M.; Hirayama, F. *J. Chem. Phys.* **1965**, *43*, 1978–1989.
(38) Persson, B. N. J.; Lang, N. D. *Phys. Rev. B* **1982**, *26*, 5409–5415.
(39) Freeman, R.; Finder, T.; Willner, I. *Angew. Chem., Int. Ed.* **2009**, *48*, 7818–7821.
(40) Li, M.; Cushing, S. K.; Wang, Q.; Shi, X.; Hornak, L. A.; Hong, Z.; Wu, N. Q. *J. Phys. Chem. Lett.* **2011**, *2*, 2125–2129.
(41) Miyake, Y.; Togashi, H.; Tashiro, M.; Yamaguchi, H.; Oda, S.; Kudo, M.; Tanaka, Y.; Kondo, Y.; Sawa, R.; Fujimoto, T.; Machinami, T.; Ono, A. *J. Am. Chem. Soc.* **2006**, *128*, 2172–2173.
(42) Jennings, T. L.; Singh, M. P.; Strouse, G. F. *J. Am. Chem. Soc.* **2006**, *128*, 5462–5467.
(43) Haldar, K. K.; Sen, T.; Patra, A. *J. Phys. Chem. C* **2010**, *114*, 4869–4874.